Time-dependent compressible extrudate-swell problem with slip at the wall

Georgios C. Georgiou

Department of Mathematics and Statistics, University of Cyprus, Kallipoleos 75, P. O. Box 537, Nicosia, Cyprus

Marcel J. Crochet

Unité de Mécanique Appliquée, Université Catholique de Louvain, Bâtiment Euler 4-6, Avenue Georges Lemaitre, B-1348 Louvain-la-Neuve, Belgium

(Received 11 April 1994; accepted 22 July 1994)

Synopsis

We solve the time-dependent compressible Newtonian extrudate-swell problem with slip at the wall, in an attempt to simulate the stick-slip extrusion instability. An arbitrary nonlinear slip model relating the shear stress to the velocity at the wall is employed, such that the flow curve consists of two stable branches separated by an unstable negative-slope branch. Finite elements are used for the space discretization and a standard fully implicit scheme for the time discretization. When the volumetric flow rate at the inlet is in the unstable regime and compressibility is taken into account, self-sustained periodic oscillations of the pressure drop and of the mass flow rate at the exit are observed and the extrudate surface becomes wavy, as is the case in stick-slip instability. Results are presented for different values of the compressibility number. As compressibility is reduced, the frequency of the oscillations becomes higher, the amplitude of the pressure drop oscillations decreases, and the amplitude of the mass flow-rate oscillations decreases, whereas the amplitude and the wavelength of the free-surface waves decrease.

I. INTRODUCTION

The role of slip at the wall in extrusion instabilities has been recently demonstrated by a number of experiments [Hill *et al.* (1990); Piau *et al.* (1990); Piau and El Kissi (1992); Hatzikiriakos and Dealy (1992a)]. Various slip equations based on experimental data have been proposed in the literature [Denn (1992); Hatzikiriakos and Dealy (1992b)]. These equations express the slip velocity as a function of the wall shear stress. At constant temperature, most of the proposed equations predict a power-law relation between the wall shear stress and the slip velocity. However, of interest to this work are slip equations that exhibit a maximum and then a minimum for the wall shear stress (as a function of the slip velocity). Such empirical models have been proposed by El Kissi and Piau (1989) and Leonov (1990).

These slip models are of great importance because they provide a mechanism for the stick-slip instability. The resulting flow curves (wall shear stress versus apparent wall shear rate or pressure drop versus volumetric flow rate) consist of two stable branches

and an intermediate unstable negative-slope branch, as Pearson and Petrie (1965) showed for the Newtonian case by means of a linear stability analysis.

In a previous paper [Georgiou and Crochet (1994)], we modeled the time-dependent compressible Newtonian flow in slits using an arbitrary slip equation relating the shear stress to the slip velocity and exhibiting a maximum and a minimum. Our numerical results show the importance of compressibility: it does not considerably affect the steady-state solutions but it changes dramatically the flow dynamics. When the volumetric flow rate at the inlet is in the unstable regime, we obtain self-sustained periodic oscillations of the pressure drop and of the mass flow rate at the exit, similar to those observed with the stick-slip instability. Plotting the pressure drop versus the mass flow rate at the outlet reveals the existence of a limit cycle on the flow-curve plane. We have obtained similar results for time-dependent Newtonian flow in a tube.

In our previous paper, we have limited our study to the flow dynamics within the tube (or the slit); the boundary condition at the outlet was a standard outflow condition, without consideration of the downstream flow. In the present paper, we wish to examine the consequences of the stick-slip instability on the shape of the jet in the extrudate-swell problem. More precisely, we wish to investigate how sustained pressure and mass flow-rate oscillations in the tube affect the development of the free surface and whether the expected waviness near the lips is convected downstream. For that purpose, we need to supplement our earlier algorithm with a time-dependent free-surface calculation.

The governing equations and the boundary conditions for the time-dependent extrudate-swell problem are presented in Sec. II. In all the time-dependent runs the volumetric flow rate at the inlet is kept constant; this is equivalent to a piston-driven flow. A brief description of the finite element formulation is also given in Sec. II. We use finite elements for the space discretization and a fully implicit scheme for the time discretization. The unknown position of the free surface is computed within the implicit scheme. In Sec. III, we study an initial-value problem where the flow moves from the steady-state stick-slip solution to that of the extrudate-swell problem. Even in the unstable regime, compressibility, acting as the storage of elastic energy, is required for generating an oscillatory flow in the tube. The oscillations of the mass flow rate in the tube then result in the waviness of the free surface. In Sec. IV, we study the effect of compressibility on the amplitude and the wavelength of the free surface. As the compressibility is decreased, the amplitude and the wavelength of the free-surface waves decrease. The conclusions are summarized in Sec. V.

II. GOVERNING EQUATIONS AND NUMERICAL METHOD

The geometry of the round extrudate-swell problem is shown in Fig. 1. If ρ, p, $\mathbf{v}$, and σ are the density, the pressure, the velocity vector, and the stress tensor, respectively, the continuity and the momentum equations for time-dependent compressible viscous flow in the absence of body forces are as follows:

$$\frac{\partial \rho}{\partial t} + \nabla \cdot \rho \mathbf{v} = 0, \tag{1}$$

$$\rho \frac{\partial \mathbf{v}}{\partial t} + \rho \mathbf{v} \cdot \nabla \mathbf{v} - \nabla \cdot \sigma = \mathbf{0}. \tag{2}$$

If the bulk viscosity is neglected, the stress tensor for compressible Newtonian flow is given by

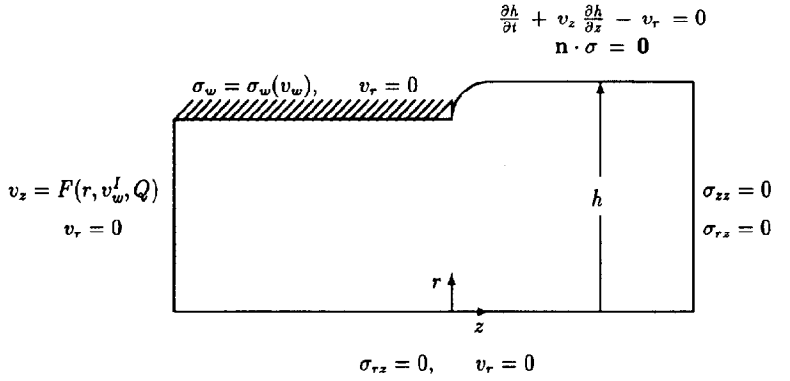

FIG. 1. Boundary conditions for the time-dependent compressible extrudate-swell problem with slip at the wall.

$$\sigma = -p(\rho)\mathbf{I} + \eta[(\nabla \mathbf{v}) + (\nabla \mathbf{v})^T] - \tfrac{2}{3}\eta \mathbf{I} \nabla \cdot \mathbf{v}, \tag{3}$$

where $\mathbf{I}$ is the unit tensor, η the viscosity, and the superscript T denotes the transpose. The viscosity is assumed to be independent of the pressure.

The above equations are completed by an equation of state relating the pressure to the density. We use the first-order expansion:

$$\rho = \rho_0[1 + \beta(p - p_0)], \tag{4}$$

where $\beta = -(1/V_0)\,(\partial V/\partial p)_{p_0, T}$ is the isothermal compressibility, ρ_0 and V_0 the density and the specific volume at the reference pressure p_0, and T the temperature.

As in Georgiou and Crochet (1994), we assume that slip occurs along the wall according to an arbitrary slip law which relates the shear stress on the wall to the relative velocity of the fluid with respect to the wall:

$$\sigma_w = \alpha_1 \left(1 + \frac{\alpha_2}{1 + \alpha_3 v_w^2}\right) v_w, \tag{5}$$

where σ_w is the shear stress exerted by the fluid on the wall, v_w the relative velocity of the fluid with respect to the wall, and α_1, α_2, α_3 material parameters. Equation (5) exhibits a maximum of σ_w provided that the dimensionless parameter α_2 is larger than 8.

It is convenient to work with dimensionless equations. To nondimensionalize the governing equations, we scale the lengths by the radius of the tube R, the velocity by a characteristic velocity V, the pressure $(p - p_0)$ and the stress components by $\eta V/R$, the density by ρ_0, and the time by R/V. We obtain five dimensionless numbers, the Reynolds number Re, a compressibility number B, and three numbers associated with the material parameters of the slip equation:

$$\mathrm{Re} \equiv \frac{\rho_0 V R}{\eta}, \quad B \equiv \frac{\beta \eta V}{R}, \quad A_1 \equiv \frac{\alpha_1 R}{\eta}, \quad A_2 \equiv \alpha_2, \quad A_3 \equiv \alpha_3 V^2. \tag{6}$$

The dimensionless forms of the equations are used hereafter.

The boundary conditions are shown in Fig. 1. Along the axis of symmetry we have the usual symmetry conditions. Along the wall, the radial velocity vanishes whereas the axial

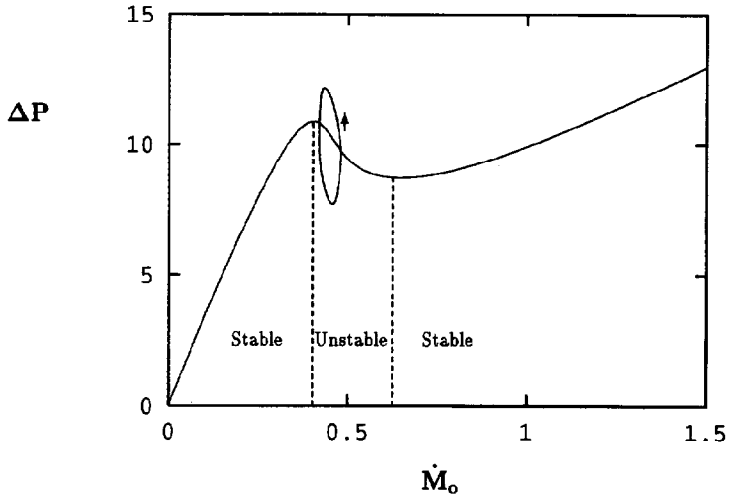

FIG. 2. Pressure drop as a function of the mass flow rate for compressible flow with slip at the wall; the nondimensional parameters are: $B = 0.01$, Re = 1, and $\Delta L = 5$. The closed curve shows a limit cycle.

velocity satisfies Eq. (5). The end of the jet is stress-free. In the absence of surface tension, we impose vanishing normal and tangential stresses on the surface of the jet. Additionally, the unknown position $h(z,t)$ of the free surface satisfies the kinematic condition:

$$\frac{\partial h}{\partial t} + v_z \frac{\partial h}{\partial z} - v_r = 0. \tag{7}$$

Finally, at the inlet plane we assume that the density is uniform (and unknown) and that the axial velocity is parabolic. The above assumptions are consistent with the analytical solution for compressible Poiseuille flow [see Georgiou and Crochet (1994) where the relevant equations are given].

We use the finite element formulation for solving the time-dependent free-surface problem. The unknown position of the free surface is calculated together with the velocity and pressure fields. Furthermore, the density is eliminated by means of the equation of state (4). We use the standard biquadratic-velocity ($P^2 - C^0$) and bilinear-pressure ($P^1 - C^0$) elements with a quadratic representation for the position h of the free surface. For the spatial discretization of the problem, we use the Galerkin forms of the continuity, momentum, and kinematic equations. For the time discretization, we use the standard fully implicit (Euler backward-difference) scheme. Special care is needed for calculating the time derivatives of $\mathbf{v}$ and p, since the finite element mesh deforms with the motion of the free surface [see, e.g., Lynch and Gray (1980)].

III. COMPRESSIBLE AND INCOMPRESSIBLE FLOW

In order to demonstrate the consequences of compressibility on the (time-dependent) free-surface problem, let us first study the evolution of the flow with a particular type of initial conditions. We start from the classical fully developed stick-slip problem: The boundary conditions are the same as those of Fig. 1, except that the kinematic condition

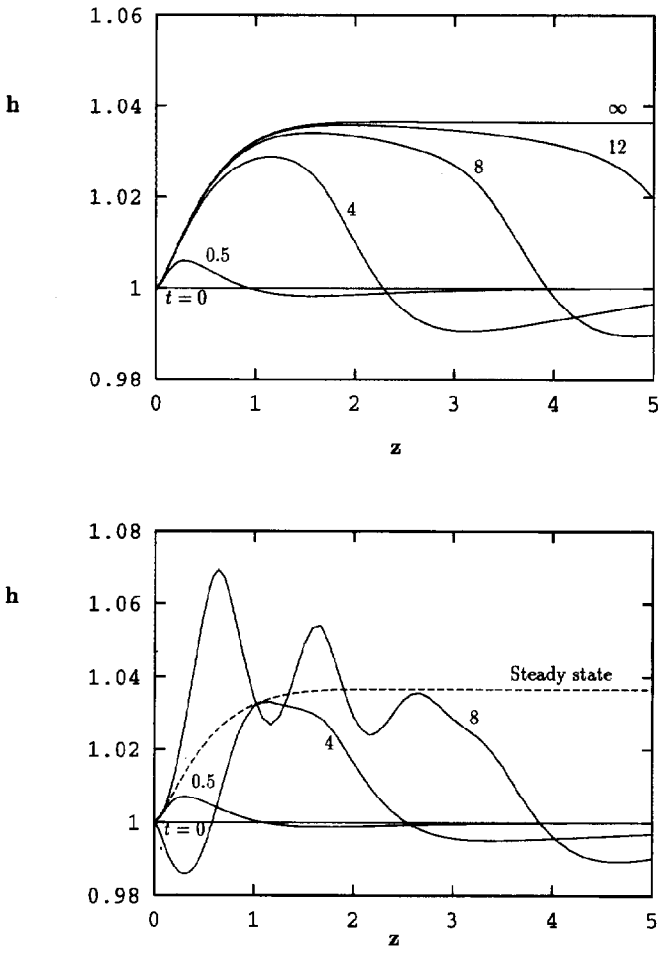

FIG. 3. Evolution of the free surface from the stick-slip to the extrudate-swell solution when the imposed volumetric flow rate falls into the unstable regime; (a) incompressible flow: the free surface does not exhibit an oscillatory behavior; (b) compressible flow ($B = 0.01$): waves propagate from the lip onwards; slip at the wall, Re = 1, $\Delta L = 5$, and $\Delta t = 0.05$.

does not apply since there is no free surface. At time $t = 0$, we activate the kinematic condition and let the free surface move to the extrudate-swell configuration while the volumetric flow rate at the inlet is kept constant.

In the present calculations, the inflow plane is taken at 5 radii upstream the exit. The length of the jet is also 5 radii. The mesh consists of 72×10 elements. The pressure drop ΔP is the value of the pressure at the intersection of the inflow plane and the wall. The dimensionless slip numbers are the same as those used in Georgiou and Crochet (1994): $A_1 = 1$, $A_2 = 20$, and $A_3 = 100$. The flow curve for Re = 1 and $B = 0.01$ is shown in Fig. 2. Note that in all the results of this paper, the mass flow rates are divided by π. Due to the particular choice of A_2 the flow curve exhibits a maximum and a minimum.

We first study the evolution of the solution when we start from the steady *incompressible* stick-slip problem with nonlinear slip at the wall. The mass flow rate at $t = 0$ is in

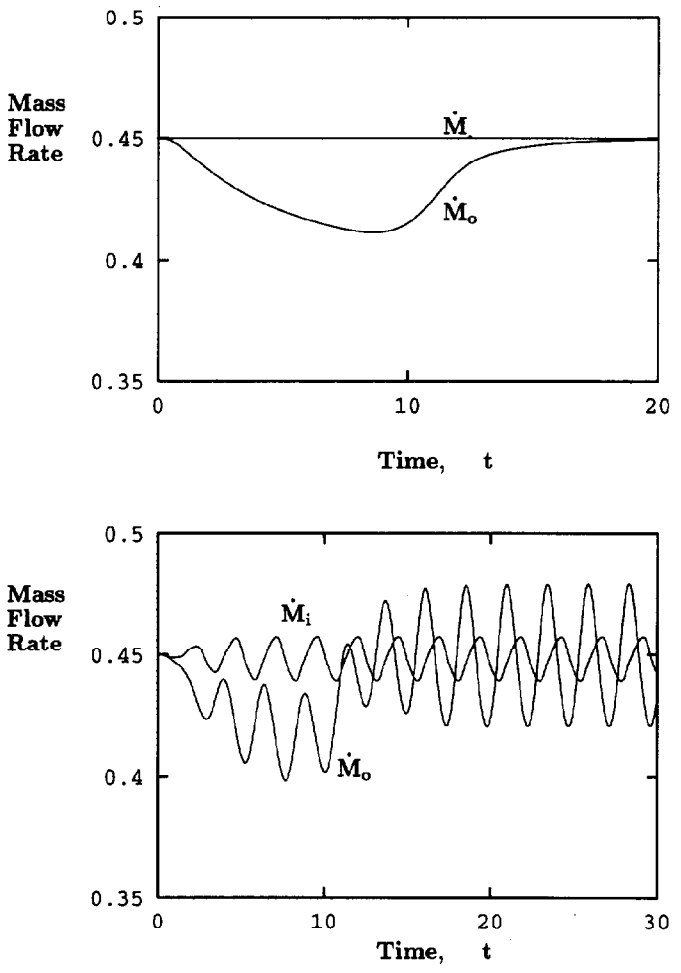

FIG. 4. Evolution of the mass flow rates at inlet ($\dot{M}_i$) and outlet ($\dot{M}_o$) from the stick-slip to the extrudate-swell solution when the imposed volumetric flow rate falls into the unstable regime; (a) incompressible flow: once the free surface reaches its steady-state configuration, $\dot{M}_i = \dot{M}_o$; (b) compressible flow ($B = 0.01$): $\dot{M}_i$ and $\dot{M}_o$ are eventually periodic with the same mean value; slip at the wall, Re = 1, $\Delta L = 5$, and $\Delta t = 0.05$.

the negative-slope regime: $\dot{M}_i = 0.45$. In Fig. 3(a), we show the evolution of the free surface from its initial configuration to the extrudate-swell solution. No oscillations are observed; we note that the eventual swelling is reduced as a consequence of slip; we recall that for a Newtonian incompressible fluid without slip at the wall, the swelling ratio is approximately 1.13. In Fig. 4(a), we show the evolution of the mass flow rates at the inflow ($\dot{M}_i$) and at the outflow ($\dot{M}_o$) planes. $\dot{M}_o$ is always below $\dot{M}_i$ because the fluid accumulates in the domain as the free surface moves to the steady extrudate-swell solution. Quite clearly, in the absence of elastic energy storage, such as that occurring with compressibility, the nonlinear character of the slip law does not lead to a periodic flow in the tube, and thus no free-surface oscillations are observed.

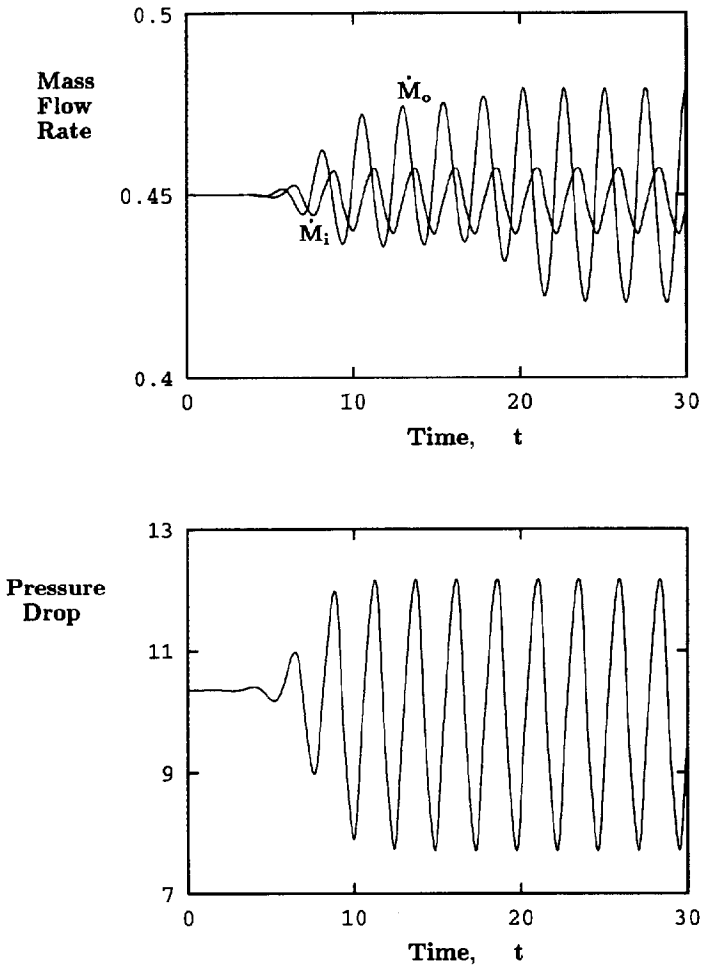

FIG. 5. Evolution of the solution when an unstable steady-state solution of the compressible extrudate-swell problem ($B = 0.01$) is slightly perturbed: (a) The mass flow rates at inlet ($\dot{M}_i$) and outlet ($\dot{M}_o$) become periodic with the same mean value, after a transient period; (b) The pressure drop shows the same periodicity; slip at the wall, Re = 1, $\Delta L = 5$, and $\Delta t = 0.01$.

We now proceed to compressible flow with slip at the wall; we select the same nondimensional parameters as in the previous flow except that, this time, $B = 0.01$. We know that typical values of the compressibility number in practical extrusion applications are much lower (i.e., of the order of $B = 0.0003$). The reason why we select a value of 0.01 in the present flow will be discussed in Sec. IV. When compressibility is taken into account, oscillatory flows are obtained when the mass flow rate falls into the unstable regime. Figure 3(b) shows that, instead of moving towards the (unstable) steady-state solution, the free surface becomes wavy. Simultaneously, we observe in Fig. 4(b) that $\dot{M}_i$ and $\dot{M}_o$ become periodic after a few oscillations. More time is required for $\dot{M}_0$ to reach a periodic behavior; during the transient regime, the average $\dot{M}_0$ is below $\dot{M}_i$ because the

fluid accumulates in the extrudate region. The periodic regime is established once the waves that start at the exit of the tube reach the outflow plane of the computational domain. If we now plot in Fig. 2 the pressure drop ΔP vs $\dot{M}_0$ after the periodic solution is established, we obtain a limit cycle similar to those obtained for Poiseuille flow in our earlier paper.

We conclude that a nonlinear slip law and inertia are not sufficient for generating a periodic flow in the tube and thus an oscillatory free surface in the extrudate-swell problem. Figures 2 and 4 show that a slight compressibility of the fluid triggers dramatic changes of behavior.

IV. THE EFFECT OF COMPRESSIBILITY

In order to examine the effect of the magnitude of the compressibility number B and to study in more detail the periodic behavior of the flow, we start from a different initial condition. As in our previous paper, we consider the steady *extrudate-swell* solution in the unstable regime and we slightly perturb the volumetric flow rate; the perturbation ΔQ equals 0.0001 Q.

Let us once more consider the case $B = 0.01$; the other parameters are the same as in Sec. III. In Fig. 5, we plot $\dot{M}_i$, $\dot{M}_o$, and ΔP as functions of time. The slight perturbation occurs at time $t = 0$. It takes about five nondimensional time units before the flow starts deviating from the steady-state (unstable) solution. As we might expect, $\dot{M}_i$ and ΔP become periodic much earlier than $\dot{M}_o$. The periodic behavior of $\dot{M}_o$ is only attained once the waviness of the free surface has reached the outflow section. The flow finally becomes periodic with the limit cycle shown in Fig. 2.

In Fig. 6, we show the motion of the free surface during one cycle, after the establishment of the periodic flow. The cycle of Fig. 6 starts at a pressure-drop minimum. It is interesting to observe that the velocity of the surface waves can be calculated through the motion of the crest point A of Fig. 6, since the deformed jet moves as a rigid body beyond a distance of about 3 radii from the lip of the die. During a period T, it can be verified that the axial displacement of A is given by $T\,\dot{M}_{o,\,\max}/r_A^2$ with the understanding that the density ρ takes the unit value in the jet. We have verified that our predictions remain unchanged when the length of the jet is 10 radii instead of 5.

We have calculated the same flow with a higher ($B = 0.02$) and a lower ($B = 0.005$) compressibility, while the other parameters remain the same. In Fig. 7, we compare the established periodic free-surface profiles observed at the time when the pressure drop is a minimum. The values of the period T of the pressure drop oscillations and of the wavelength λ of the free surface are listed in Table I. As in Georgiou and Crochet (1994), we observe that as compressibility decreases, the frequency of the oscillations becomes higher, the amplitude of the pressure-drop oscillations decreases, and the amplitude of the mass flow-rate oscillations decreases. As expected, the amplitude and the wavelength of the free-surface waves decrease as B decreases.

These observations constitute the reason why, in our present developments, we limit our calculations to values of B not lower than 0.005. On one hand, lower values of B would require much finer finite element meshes for simulating the generation of small wavelengths in the free surface; on the other hand, the presence of viscoelasticity would enhance the amplitude of the surface waves.

V. CONCLUSIONS

We have solved the time-dependent compressible Newtonian extrudate-swell problem with slip at the wall, using finite elements in space and a fully implicit scheme for the

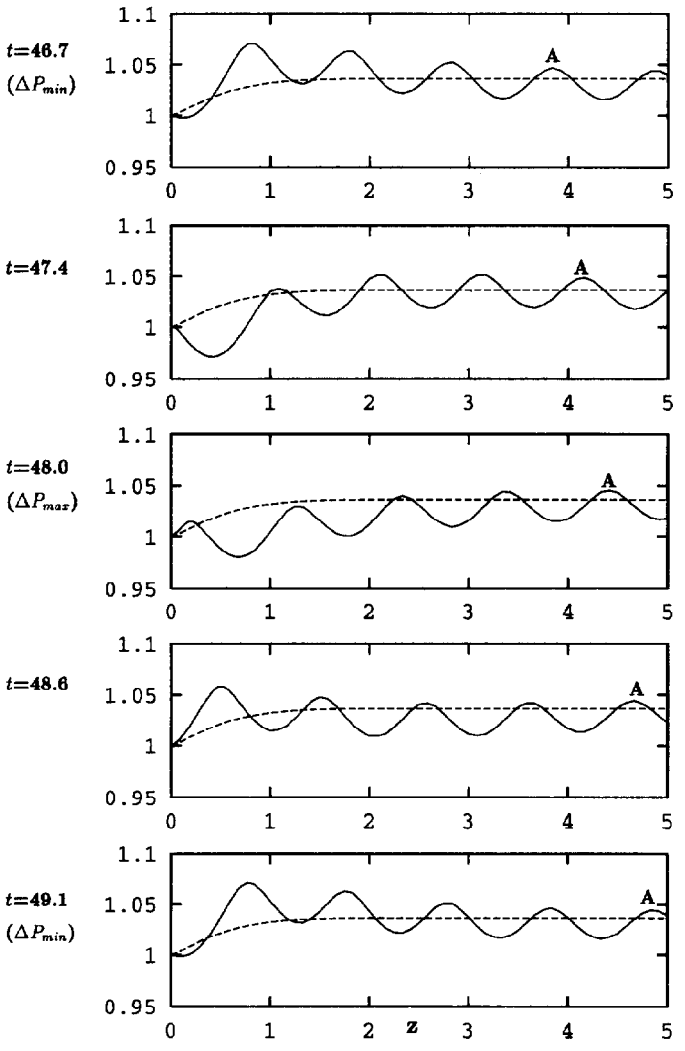

FIG. 6. Successive configurations of the free surface throughout a cycle of the established periodic solution of Fig. 5; the dotted line shows the (unstable) steady-state configuration.

time discretization. The synergy of nonlinear slip and compressibility results in the generation of self-sustained periodic oscillations of the pressure drop and of the mass flow rate in the die, in an intermediate range of volumetric flow rates. The oscillatory flow in the die causes the oscillations of the free surface to become wavy, as is the case in the stick-slip instability. The amplitude and the wavelength of the free-surface waves decrease as compressibility is reduced.

One may wonder whether compressibility is a necessary condition for the waviness of the free surface. Such waviness requires an oscillatory volumetric flow rate in the exit section of the die. We have shown that such an oscillation may be the result of the

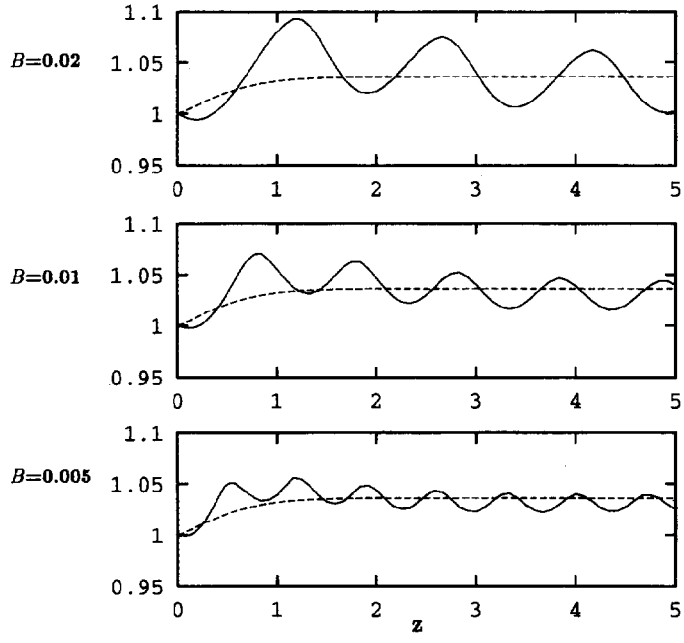

FIG. 7. Free-surface profiles obtained for three different values of the compressibility coefficient B; the amplitude and the wavelength of the oscillations decrease as B decreases. The dotted lines show the (unstable) steady-state configurations; slip at the wall, Re = 1 and $\Delta L = 5$.

combination of nonlinear slip and compressibility. However, other mechanisms may as well lead to the same effect, even for an incompressible fluid. In the case of an incompressible viscoelastic fluid, the combination of elasticity and of nonlinear slip may very well lead to oscillatory flow rate and consequently to a wavy free surface.

Further progress requires the use of more realistic constitutive equations for the fluid and for the nonlinear slip model.

ACKNOWLEDGMENTS

This paper presents research results of the Belgian Programme on Interuniversity Poles of Attraction, initiated by the Belgian State, Prime Minister's Office for Science, Technology and Culture. The scientific responsibility rests with its authors.

TABLE I. Approximate values of the period of the pressure-drop oscillations (T) and of the wavelength (λ) of the free-surface waves.

B	T	λ
0.02	3.63	1.5
0.01	2.44	1.0
0.005	1.67	0.7

References

Denn, M. M., "Surface-induced effects in polymer melt flow," in *Theoretical and Applied Rheology*, edited by P. Moldenaers and R. Keunings (Elsevier Science, New York, 1992), pp. 45–49.

El Kissi, N., and J. M. Piau, "Ecoulement de fluides polymères enchevêtrés dans un capillaire. Modélisation du glissement macroscopique à la paroi," C. R. Acad. Sci. Paris **309**, 7–9 (1989).

Georgiou, G. C. and M. J. Crochet, "Compressible viscous flow in slits, with slip at the wall," J. Rheol. **38**, 639–654 (1994).

Hatzikiriakos, S. G. and J. M. Dealy, "Wall slip of molten high density polyethylenes. II. Capillary rheometer studies," J. Rheol. **36**, 703–741 (1992a).

Hatzikiriakos, S. G. and J. M. Dealy, "Role of slip and fracture in the oscillating flow of HDPE in a capillary," J. Rheol. **36**, 845–884 (1992b).

Hill, D. A., T. Hasegawa, and M. M. Denn, "On the apparent relation between adhesive failure and melt fracture," J. Rheol. **34**, 891–918 (1990).

Leonov, A. I., "On the dependence of friction force on sliding velocity in the theory of adhesive friction of elastomers," Wear **141**, 137–145 (1990).

Lynch, D. R. and W. G. Gray, "Finite element simulation of flow in deforming regions," J. Comput. Phys. **36**, 135–153 (1980).

Pearson, J. R. A. and C. J. S. Petrie, "On the melt-flow instability of extruded polymers," Proc 4th Int. Rheol. Cong. **3**, 265–282 (1965).

Piau, J. M., N. El Kissi, and B. Tremblay, "Influence of upstream instabilities and wall slip on melt fracture and sharkskin phenomena during silicones extrusion through orifice dies," J. Non-Newt. Fluid Mech. **34**, 145–180 (1990).

Piau, J. M. and N. El Kissi, "The influence of interface and volume properties of polymer melts on their die flow stability," in *Theoretical and Applied Rheology*, edited by P. Moldenaers and R. Keunings (Elsevier Science, New York, 1992), pp. 70–74.